The Journal of Clinical Endocrinology & Metabolism, 2021, Vol. 106, No. 10, 2901–2914
https://doi.org/10.1210/clinem/dgab447
Clinical Research Article

Clinical Research Article

Brown Adipose Tissue, Adiposity, and Metabolic Profile in Preschool Children

Mya Thway Tint,[1,2] Navin Michael,[1] Suresh Anand Sadananthan,[1] Jonathan Yinhao Huang,[1] Chin Meng Khoo,[3] Keith M. Godfrey,[4,5] Lynette Pei-Chi Shek,[6] Ngee Lek,[7] Kok Hian Tan,[8] Fabian Yap,[7,9,10] S. Sendhil Velan,[1,11] Peter D. Gluckman,[1,12] Yap-Seng Chong,[1,2] Neerja Karnani,[1,13] Shiao-Yng Chan,[1,2] Melvin Khee-Shing Leow,[1,14,15,16] Kuan Jin Lee,[11] Yung-Seng Lee,[1,6,17] Houchun Harry Hu,[18] Cuilin Zhang,[19] Marielle V. Fortier,[1,20] and Johan G. Eriksson[1,2,21,22]

[1]Singapore Institute for Clinical Sciences (SICS), Agency for Science, Technology and Research (A*STAR), Singapore; [2]Department of Obstetrics & Gynecology, Yong Loo Lin School of Medicine, National University of Singapore, Singapore; [3]Division of Endocrinology, Department of Medicine, National University Health System, Singapore; [4]MRC Lifecourse Epidemiology Unit, University of Southampton, Southampton, UK; [5]NIHR Southampton Biomedical Research Centre, University Hospital Southampton, NHS Foundation Trust, Southampton, UK; [6]Department of Paediatrics, Yong Loo Lin School of Medicine, National University of Singapore, Singapore; [7]Department of Pediatric Endocrinology, KK Women's and Children's Hospital, Singapore; [8]Department of Obstetrics and Gynaecology, KK Women's and Children's Hospital, Singapore; [9]Duke-NUS Graduate Medical School, Singapore; [10]Lee Kong Chian School of Medicine, Nanyang Technological University, Singapore; [11]Singapore Bioimaging Consortium (SBIC), Agency for Science, Technology and Research (A*STAR), Singapore; [12]Liggins Institute, University of Auckland, Auckland, New Zealand; [13]Department of Biochemistry, Yong Loo Lin School of Medicine, National University of Singapore, Singapore; [14]Department of Endocrinology, Tan Tock Seng Hospital, Singapore; [15]Metabolic Disorders Research Programme, Lee Kong Chian School of Medicine, Singapore; [16]Cardiovascular and Metabolic Disorders Program, Duke-NUS Medical School, Singapore; [17]Division of Paediatric Endocrinology, Department of Paediatrics, Khoo Teck Puat–National University Children's Medical Institute, National University Health System, Singapore; [18]Department of Radiology, Nationwide Children's Hospital, Columbus, OH, USA; [19]Epidemiology Branch, Division of Intramural Population Health Research, Eunice Kennedy Shriver National Institute of Child Health and Human Development, National Institutes of Health, Rockville, MD, USA; [20]Department of Diagnostic and Interventional Imaging, KK Women's and Children's Hospital, Singapore; [21]Department of General Practice and Primary Health Care, University of Helsinki and Helsinki University Hospital, Helsinki, Finland; and [22]Folkhälsan Research Center, Helsinki, Finland

ORCiD numbers: 0000-0002-9548-7186 (M. Thway Tint); 0000-0002-6170-2108 (N. Michael); 0000-0002-7232-8473 (Y.-S. Chong), 0000-0002-2516-2060 (J. G. Eriksson).

Received: 9 February 2021; Editorial Decision: 14 June 2021; First Published Online: 18 June 2021; Corrected and Typeset: 23 July 2021.

ISSN Print 0021-972X ISSN Online 1945-7197
Printed in USA

Abstract

Context: An inverse relationship between brown adipose tissue (BAT) and obesity has previously been reported in older children and adults but is unknown in young children.
Objective: We investigated the influence of BAT in thermoneutral condition on adiposity and metabolic profile in Asian preschool children.
Design, Setting, and Participants: A total of 198 children aged 4.5 years from a prospective birth cohort study, Growing Up in Singapore Towards Healthy Outcomes (GUSTO) were successfully studied with water-fat magnetic resonance imaging of the supraclavicular and axillary fat depot (FD_{SA}). Regions within FD_{SA} with fat-signal-fraction between 20% and 80% were considered BAT, and percentage BAT (%BAT; 100*BAT volume/ FD_{SA} volume) was calculated.
Main Outcome Measures: Abdominal adipose tissue compartment volumes, ectopic fat in the soleus muscle and liver, fatty liver index, metabolic syndrome scores, and markers of insulin sensitivity.
Results: A 1% unit increase in %BAT was associated with lower body mass index, difference (95% CI), –0.08 (–0.10, –0.06) kg/m^2 and smaller abdominal adipose tissue compartment volumes. Ethnicity and sex modified these associations. In addition, each unit increase in %BAT was associated with lower ectopic fat at 4.5 years in the liver, –0.008% (–0.013%, –0.003%); soleus muscle, –0.003% (–0.006%, –0.001%) of water content and lower fatty liver index at 6 years.
Conclusions: Higher %BAT is associated with a more favorable metabolic profile. BAT may thus play a role in the pathophysiology of obesity and related metabolic disorders. The observed ethnic and sex differences imply that the protective effect of BAT may vary among different groups.

Key Words: brown fat, adiposity, metabolic profile, preschool children

Adipose tissue is commonly divided into white (WAT) and brown adipose tissue (BAT). WAT is commonly thought to be a storage depot for energy and an endocrine organ secreting adipokines including adiponectin and leptin. BAT is suggested to be a major contributor to the regulation of energy metabolism (1). BAT, when activated, increases thermogenesis by stimulating fatty acid oxidation through mitochondrial uncoupling protein-1 and increases energy dissipation (1,2). BAT also possesses a great capacity for glucose uptake from the circulation thereby improving insulin sensitivity by both insulin-dependent and insulin-independent pathways (3,4). These properties suggest that BAT has a role in whole-body metabolism. Therefore BAT has recently received a great deal of attention as a potential target for obesity therapy (4). There seems to be a major crosstalk between several organs including BAT, liver, skeletal muscle, and gut as well as the central nervous system in regulation of energy metabolism Originally, BAT was believed to be present only in infancy, but it is now known to persist into childhood and adulthood (5-8). Cold-induced activated BAT is inversely related to body mass index (BMI), obesity, and visceral fat in older children and adults (9-11). However, such associations have been little explored in younger children. The most commonly used method for estimating BAT activity in humans has been 18F-fluorodeoxyglucose (FDG) positron emission tomography (PET) combined with computed tomography (CT), which exposes subjects to significant doses of ionizing radiation and thus its applicability to the general population, its use in children, and in large cohort studies is limited. More important, recent studies have highlighted that PET/CT may underestimate the amount of BAT as PET/CT can only detect activated BAT, generally by cold- or pharmacologically induced activation (12-14). The increased uptake of the most commonly used glucose tracer (eg, FDG) is used as the indication of activated BAT during PET/CT scans. Therefore, BAT with FDG uptake below the detection limit or nonactivated BAT are less likely to be detected by PET/CT scans. Recently, a multiecho chemical-shift water-fat magnetic resonance imaging (MRI) was introduced as an alternative imaging technique to PET/CT in detecting BAT without requiring physiological activation. Water-fat MRI is capable of detecting BAT under thermoneutral conditions without the use of ionizing radiation (15-17). Therefore, this study aimed to examine the association of nonactivated BAT, quantified using water-fat MRI, with

metabolic parameters. Total and abdominal adiposity and ectopic fat in the liver and soleus muscle measured at 4.5 years were primary outcomes, and fatty liver index (FLI), metabolic syndrome (MetS) score, and measures of insulin resistance, fasting plasma glucose (FPG), and insulin measured at 6 years were secondary outcomes.

Materials and Methods

Subjects

Children who participated were from the Growing up in Singapore Toward Healthy Outcomes (GUSTO), a prospective observational mother-offspring birth cohort study (18). GUSTO was set up to evaluate the developmental influences on the risk of metabolic diseases. This study was approved by the institutional review board of the Singapore National Healthcare Group and the Central Institutional Review Board of SingHealth. Between June 2009 and September 2010, 1450 pregnant women were recruited during the first trimester of pregnancy. To be eligible in GUSTO study, mothers had to be aged 18 years and above, intended to deliver in 1 of the 2 main public maternity units in Singapore; the KK Women's and Children's Hospital or the National University Hospital, and to reside in Singapore for the next 5 years. Pregnant women self-identified their homogenous ethnicity; Chinese, Malay or Indian (ie, same ethnicity of the subject, their partners, and both sides of parents). Study visits for metabolic imaging were conducted from June 2015 to December 2016 when the children were 4.5 years old. MRI was offered to the parents of all participants and performed on children whose parents provided written informed consents. After quality control procedures for good image quality and symmetric body positioning, 198 of the 330 children with water-fat MRI were included in the analyses. A priori sample size calculations were not performed as we considered this study an exploratory comparison between BAT and metabolic profile in children. Figure 1 shows the study flow chart.

Magnetic Resonance Imaging: Image Acquisition, Segmentation, and Quantification

Image acquisition

MRI was performed on a 3T MR scanner (Magnetom Skyra, Siemens Healthcare, Erlangen, Germany) without sedation or any form of BAT stimulation at a room temperature between 20° to 22°C and a minimum of 3 to 5 h after afternoon meals. MR scans were taken with children in supine position with arms abducted. A multiecho chemical-shift–based water-fat MRI sequence of supraclavicular and axillary fat depots (FD_{SA}) with flexible echo times (TE) was acquired (15). FD_{SA} is the main location of BAT after infancy

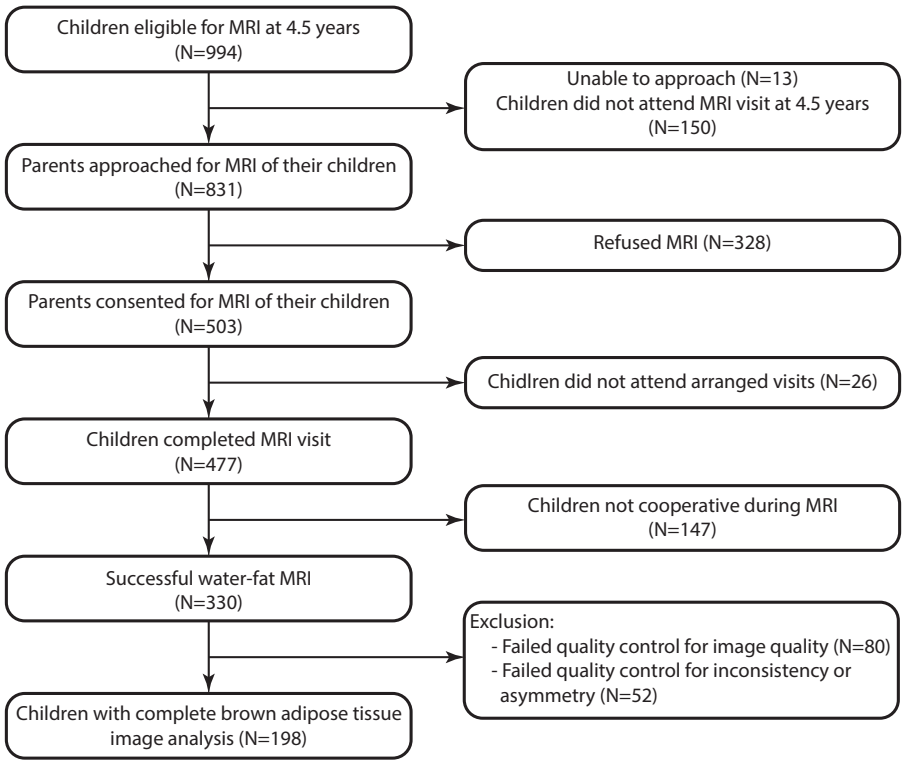

Figure 1. Study flow chart showing children participating in MRI at 4.5 years.

and anatomically easily identifiable and has been extensively studied in humans using PET/CT scans. Pertinent sequence parameters included 104 axial slices with 1.6-mm thickness and in-plane resolution of 1.6 × 1.6 mm; repetition time: 10 msec; TEs: 1.00, 2.41, 3.82, 5.23, 6.64, and 8.05 msec; flip angle: 5° covering the region from the base of the neck to the inferior border of the scapula.

Segmentation of BAT

All 3 planes of MR images (axial, coronal, and sagittal) were utilized in defining FD_{SA}. The first step was the contouring of FD_{SA}, which was performed following anatomical boundaries. The superior border was the base of the neck above the clavicular head, with other borders defined inferiorly by the axillary fold, medially (anteriorly) by the sternocleidomastoid muscle and posteriorly (laterally) by the anterior border of the trapezius muscle or the scapula. Regions of interest were drawn in the stack of slices of the supraclavicular-axillary region from which the averaged signal intensities were calculated within each region of interest subsequently.

The next step was the manual optimizing process. The consistency and quality of the manual optimization were validated by repeating the procedure twice on randomly selected 20 data sets and measuring the inter- and intrarater reliability (Table 1). The mean dice similarity coefficients (DSC) for intra- and interrater reliability for BAT were 0.85 and 0.86, respectively. The DSC is used to quantify the performance of image segmentation and is a measure of how similar the objects are (19). It is the size of the overlap of the 2 segmentations divided by the total size of the 2 objects. The DSC is not only a measure of true positives, but it also penalizes the false positives that the method finds, similar to precision. The DSC ranges between 0 and 1 and scores greater than 0.7 can be interpreted as a high grade of overlap of the generated contours.

Table 1. Intra- and Interreliability of manual segmentation of brown adipose tissue

	Dice similarity coefficients	
Subject	Intrareliability	Interreliability
1	0.83	0.85
2	0.80	0.86
3	0.89	0.91
4	0.85	0.90
5	0.83	0.82
6	0.88	0.87
7	0.83	0.87
8	0.87	0.82
9	0.88	0.84
10	0.76	0.85
11	0.89	0.90
12	0.89	0.86
13	0.79	0.82
14	0.88	0.87
15	0.85	0.90
16	0.83	0.85
17	0.85	0.85
18	0.76	0.80
19	0.86	0.86
20	0.87	0.90

Dice similarity coefficients are not only a measure of true positives but also penalize for the false positives. The Dice similarity coefficients range between 0 and 1 and scores greater than 0.7 can be interpreted as a high grade of overlap of the generated contours.

Quantification of BAT

Chemical-shift water fat MRI is capable of generating distinct signal contrasts between BAT and WAT. Water-fat MRI provides spatially resolved fat-signal fraction (FF) maps, which are proportional to the fat content within voxels in FD_{SA} ranging from 0% to 100%. BAT and WAT were differentiated by exploiting their inherent differences in FF. In vivo BAT from FF maps in infants and children identified by water-fat MRI has been and validated against CT and dissection, and the depots have been verified as BAT using histological and biochemical analysis.(15,16). WAT regions have increased signal intensities and are predominantly composed of lipids and thus has a low water to fat ratio. In contrast, BAT depots exhibited intermediate gray signal intensities, suggesting a high water-to-fat ratio compared to WAT. The regions within FD_{SA} with FF between 20% and 80% were used as a proxy for estimating BAT (12,16) while regions within FD_{SA} with FF between 81% to 100% were defined as WAT. The initial manual delineation and segmentation of bilateral FD_{SA} were performed by 2 trained image analysts using ITK-SNAP (www.itksnap.org) followed by optimization, and final review was done by a pediatric radiologist. All analysts were blinded to participant information. BAT and WAT volumes for FD_{SA} were then generated by multiplying the number of respective segmented voxels by the voxel dimension (1·6 × 1·6 × 1·6) mm.

FD_{SA} depots were heterogeneous and had regions interspersed with varying degrees of FF in preschool children. Previous studies using water-fat MRI used FF as a measure of BAT. Activated BAT induces lipolysis within BAT, which subsequently depletes its triglyceride (TG) content (1) and thus increases water-to-fat ratio within BAT. FF may be reflective of BAT activity; it does not provide quantitative information about BAT deposition. In the MRI images of children in this study, characteristics of FD_{SA} is more BAT-like with lower FF in children with lower BMI while more WAT-like with higher FF in children with higher BMI (Fig. 2). In other

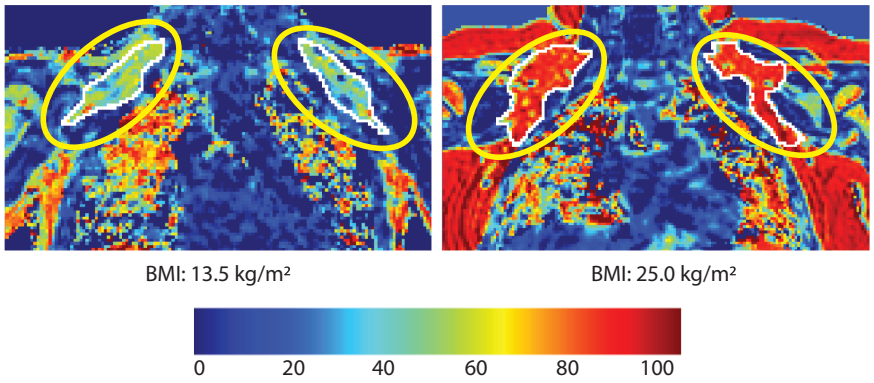

Figure 2. Color map of supraclavicular and axillary fat depots from water-fat MRI images in preschool children. Segmented supraclavicular and axillary fat depots (FD_{SA}) were indicated by white boundaries. Color map of fat-signal-fractions is illustrated on 0% (blue) to 100% (red) scale. Supraclavicular-axillary fat depots (outlined white) exhibit lower fat fractions in a child with BMI 13.5 kg/m^2 (A) *vs* a child with BMI 25.0 kg/m^2 (B).

words, children with lower BMI had lower volume of FD_{SA} with BAT characteristics, and children with higher BMI will have higher volume of FD_{SA} with mostly WAT characteristics. We thus explored a new approach to present BAT with normalization of depot size. Therefore, the proportion of BAT within FD_{SA} [100*BAT volume/FD_{SA} volume; ie, percentage BAT (%BAT) was calculated as one of the measures of BAT]. %WAT was also calculated (100*WAT volume/FD_{SA} volume). Figure 3 shows the scatter plots of the association between child's BMI and measures of adipose tissue within FD_{SA} (BAT and WAT). A positive association was observed between BMI and BAT volume while the association was inverse between BMI and %BAT. However, the associations between BMI and WAT, expressed as either volume or percentage of WAT, were both positive. These associations were similar between BMI and other adiposity measures. Therefore, BAT FF and %BAT were used as BAT measures in multivariable regression analyses.

Abdominal MRI was performed to quantify the volumes of abdominal adipose tissue compartments and superficial subcutaneous (SSAT), deep subcutaneous (DSAT), and visceral (VAT) adipose tissue using a fully automated graph theoretic segmentation algorithm and quantified as described elsewhere (20,21). Liver fat (fat content per unit of liver weight, expressed as percentage) and intramyocellular lipids (IMCL) of the soleus muscle (expressed as a percentage of tissue water content) were assessed by proton magnetic resonance spectroscopy as previously described.

Child's anthropometric measurement at 4.5 years

Height (using a SECA213 stadiometer) and weight (using a SECA803 weighing scale) were measured in duplicates. BMI was calculated as weight (kg)/height (m^2). Skinfold thicknesses (SFT; triceps, biceps, subscapular, and suprailiac) were measured on the right side of the body in triplicate using Holtain skinfold calipers (Holtain Ltd). The mean of the 2 closest measurements for height, weight, and SFT was used for analyses. Sum of SFT (ΣSFT) of all 4 sites was used as a measure of total adiposity.

Assessment of metabolic markers at 6 years

Venous blood was drawn after 8 to 10 h of fasting. FPG was measured using enzymatic hexokinase methods (Abbott Architect c8000 analyzer and Beckman AU5800 analyzer at clinical referral laboratories of KK Women's and Children's Hospital and National University Hospital, respectively). Insulin was measured using the Access ultrasensitive immunoassay (Beckman Dxl800 analyzer, Beckman Coulter). Gamma glutamyl transferase (GGT), TG, and high-density lipoprotein-cholesterol were measured using enzymatic colorimetric assay (Beckman AU5800 analyzer).

For children with available data on TG and GGT, FLI was calculated using a published equation [0.953*ln (TG) + 0.139*BMI + 0.718*ln(GGT) + 0.053*waist – 15 .745] (22). The FLI is an index to estimate nonalcoholic fatty liver disease (NAFLD) with modest efficacy compared to magnetic resonance spectroscopy (MRS), which is expensive and not readily accessible. FLI varies between 0 and 100, and a threshold of <30 can be used to rule out NAFLD. A MetS score for children was generated as the sum of sex- and age-specific *z*-scores for waist circumference and homeostatic model assessment of insulin resistance (fasting plasma insulin*FPG)/22.5, the mean of *z*-scores of diastolic and systolic blood pressure and high-density lipoprotein-cholesterol (multiplied by –1 due to its inverse association with metabolic risk), and TG (23,24). A higher score indicates a less favorable metabolic profile.

Statistical analysis

Multivariable regression analyses were used to examine the associations between %BAT and metabolic profiles in children. Primary outcome measures were total adiposity;

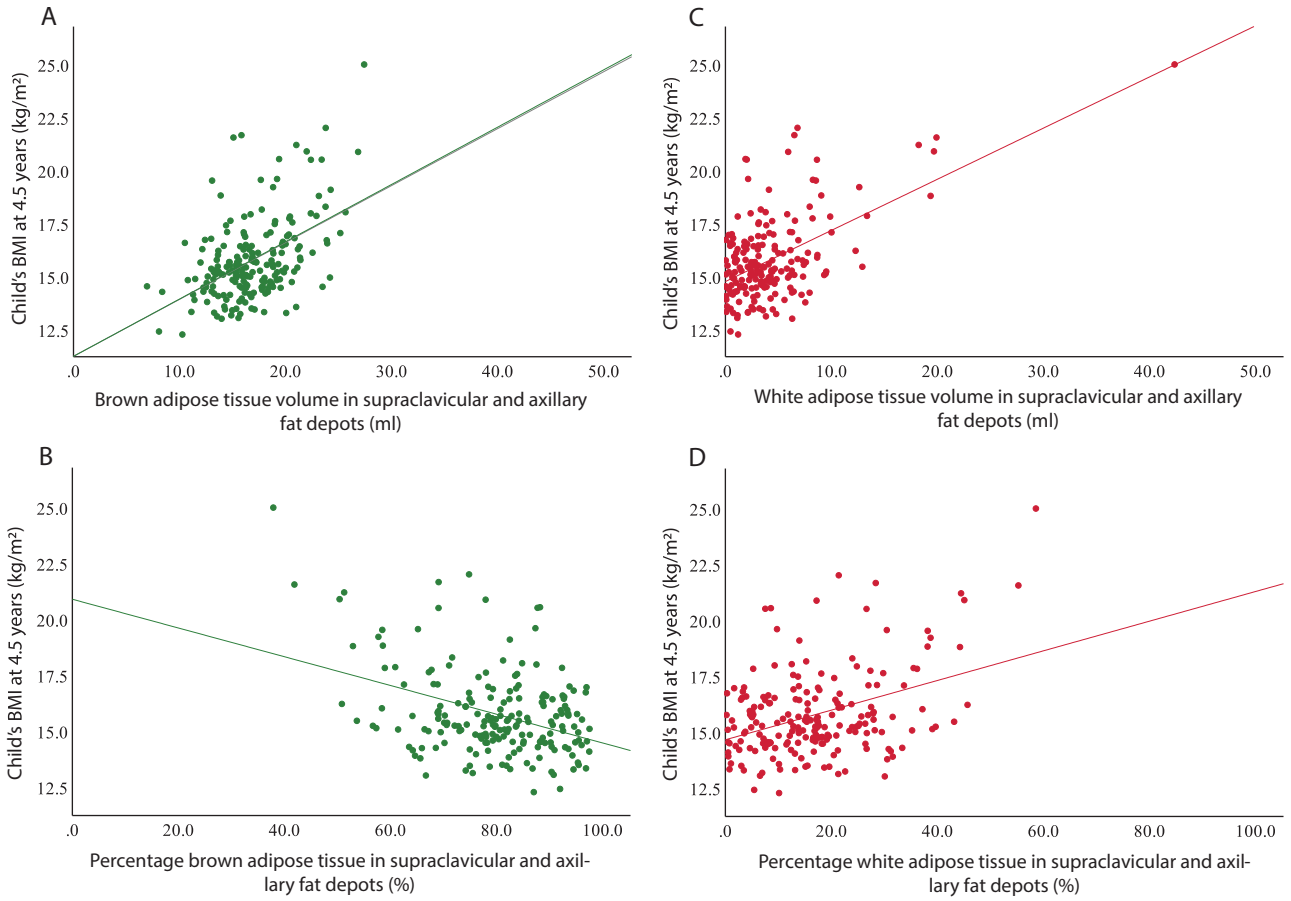

Figure 3. Scatter plots of child's body mass index and brown and white adipose tissue within supraclavicular and axillary fat depot at 4.5 years. Scatter plots of child's BMI and brown and white adipose tissue within supra-clavicular fat depot at 4.5 years. (A) The association between BMI and volume of brown adipose tissue; (B) the association between BMI and percentage of brown adipose tissue; (C) the association between BMI and volume of white adipose tissue; and (D) the association between BMI and percentage of white adipose tissue within supraclavicular and axillary fat depot.

BMI and ΣSFT; abdominal adiposity measured by abdominal adipose tissue compartment volumes; SSAT, DSAT, and VAT; ectopic fat in the liver; and IMCL in soleus muscle at age 4.5 years. Secondary outcomes were metabolic parameters: FLI, MetS score and measures of insulin resistance, FPG, and fasting plasma insulin at age 6 years. Covariates, which are shown to have associations with BAT in the literature (ie, ethnicity, child's sex and age) were controlled for in the regression analyses. Ethnicity and sex modified the associations between %BAT and adiposity, and thus stratified analyses were performed. All statistical analyses were performed using SPSS Statistics for Windows, version 21.0. (IBM Corp., Armonk, NY, USA). Two-sided *P*-values of less than 0.05 indicated statistical significance. *P*-values were corrected using Benjamini-Hockberg method with false discovery rate of 0.05 (25).

Results

The characteristics of the children of this study are shown in Table 2. There were 86 Chinese (43.4%), 66 Malay (33.3%), and 46 Indian (23.2%) children and 89 boys (44.9%) and 109 girls (55.1%). Indian and Malay children had higher %BAT compared to Chinese children. Indian children also had higher SAT and ectopic fat compared to Chinese or Malay children despite having similar BMI. Girls had higher ΣSFT and SAT and lower %BAT than boys. Following sex and age group standardized BMI cutoff points by Cole et al, 8.6% of children were overweight and 7.1% were obese (26). Generally, the participants of this study had similar characteristics with the children who completed MRI with poor image quality and GUSTO children who did not participated in this study, except that participants appeared to have lower IMCL at 4.5 years compared to those children. The participants also had marginally higher sum of SFT than the children of the whole GUSTO cohort who did not participate in this study (Table 3).

Table 4 shows that %BAT had an inverse correlation while BAT FF within FD_{SA} had a positive correlation with adiposity and all metabolic parameters, total and abdominal adiposity, ectopic fat, and FLI. Figure 2 shows as an example

Table 2. Characteristics of participants by ethnicity groups and sex

			Ethnicity			Sex	
	N	All	Chinese,	Malay	Indian	Boys	Girls
n (%)	198	198 (100.0)	86 (43.4)	66 (33.3)	46 (23.2)	89 (44.95)	109 (55.05)
Age (years)	198	4.58 (0.07)	4.57 (0.06)	4.58 (0.08)	4.59 (0.08)	4.57 (0.07)	4.59 (0.09)
Brown adipose tissue measures at 4.5 years							
Mean fat-signal-fraction of BAT within FD_{SA}	198	0.51 (0.05)	0.52 (0.04)	0.51 (0.05)	0.51 (0.05)	0.50 (0.04)	0.52 (0.05)
BAT volume within FD_{SA} (ml)	198	16.89 (3.53)	16.40 (2.95)	17.49 (3.38)	16.94 (4.55)	17.44 (3.53)	16.44 (3.48)
BAT within FD_{SA} (%)	198	79.70 (11.66)	76.88 (11.25)	81.38 (11.70)	82.54 (11.45)	82.28 (9.38)	77.59 (12.90)
Total adiposity measures at 4.5 years							
Body mass index (kg/m^2)	198	15.77 (1.94)	15.54 (1.60)	16.00 (1.65)	15.87 (2.74)	15.94 (1.74)	15.63 (2.08)
Sum of skinfold thickness (mm)	194	32.40 (12.43)	30.38 (8.14)	32.76 (11.67)	35.53 (18.19)	28.75 (9.26)	35.38 (13.86)
Abdominal adiposity measures at 4.5 years							
SSAT (mL)	187	427.20 (251.24)	391.54 (163.38)	422.94 (235.67)	499.16 (370.97)	369.45 (186.83)	472.30 (284.65)
DSAT (mL)	187	173.88 (182.84)	143.83 (118.31)	173.21 (179.81)	230.09 (260.48)	133.51 (124.25)	205.40 (213.25)
VAT (mL)	187	192.02 (86.31)	198.02 (69.68)	184.32 (60.15)	192.61 (135.27)	192.14 (72.20)	191.92 (96.24)
Ectopic fat measured by MRS at 4.5 years							
Liver fat (% of liver weight)	158	0.567 (0.364)	0.538 (0.338)	0.563 (0.354)	0.632 (0.426)	0.580 (0.362)	0.559 (0.366)
Intramyocellular lipids (% of water content)	170	0.461(0.205)	0.453(0.182)	0.428(0.174)	0.531(0.274)	0.454 (0.200)	0.466 (0.210)
Adiposity and metabolic parameters at 6 years							
Age (years)	198	6.05 (0.09)	6.05 (0.09)	6.06 (0.09)	6.04 (0.10)	6.04 (0.9)	6.06 (0.9)
Body mass index (kg/m^2)	198	15.70 (2.23)	15.38 (1.91)	16.15 (2.31)	15.67 (2.62)	15.68 (1.98)	15.73 (2.43)
Fatty liver index	84	1.100 (1.534)	1.063 (1.697)	0.926 (0.724)	1.376 (1.920)	0.773 (0.581)	1.312 (1.890)
Metabolic syndrome score	89	0.192 (2.262)	0.073 (2.371)	0.247 (1.881)	0.349 (2.264)	−0.030 (1.771)	0.328 (2.525)
Fasting plasma glucose (mmol/L)	142	4.51 (0.38)	4.54 (0.37)	4.47 (0.42)	4.53 (0.34)	4.62 (0.36)	4.43 (0.38)
Fasting plasma insulin (mU/L)	116	5.00 (3.94)	4.54 (3.25)	5.65 (5.28)	4.94 (2.60)	4.49 (3.29)	5.30 (4.27)

Data shown are N (%) for categorical variables and mean (SD) for continuous variables.
Abbreviations: BAT, brown adipose tissue; DSAT, abdominal deep subcutaneous adipose tissue; FD_{SA}, supraclavicular and axillary fat depot; SSAT, abdominal superficial subcutaneous adipose tissue; VAT, visceral adipose tissue.

that FD_{SA} exhibits lower FF in 1 child with BMI 13.5 kg/m^2, which is primarily filled with BAT, and higher FF in a child with BMI 25.0 kg/m^2, which was devoid of BAT.

Associations Between %BAT and Adiposity at Age 4.5 Years

A 1% unit increase in %BAT was associated with lower total adiposity measures: BMI, β (95% CI) −0.08 (−0.10, −0.06) kg/m^2 and ΣSFT, −0.57 (−0.70, −0.44) mm (Table 5). Similarly, each 1% unit increase in %BAT was associated with lower abdominal adiposity: SSAT −11.16 (−13.87, −8.45) mL, DSAT −8.21 (−10.17, −6.25) mL, and VAT −4.26 (−5.19, −3.32) mL (Table 5). The interaction terms were significant between %BAT and ethnicity as well as sex on total and abdominal adiposity measures. Therefore, stratified analyses by ethnicity and sex were performed. An increase in %BAT was associated with a reduction in total

Table 3. Comparison of characteristics of study participants and nonparticipants

	N	Participants	N	Children excluded due to failed image QC	P^a	N	Nonparticipants of whole GUSTO cohort	P^b
Age (years)	198	4.58 (0.07)	132	4.56 (0.07)	0.116	633	4.55 (0.08)	0.718
Total adiposity measures at 4.5 years								
Body mass index (kg/m^2)	198	15.77 (1.94)	132	15.47 (1.83)	0.589	633	15.48 (1.81)	0.372
Sum of skinfold thickness (mm)	194	32.40 (12.43)	129	29.57 (10.64)	0.232	602	30.34 (10.02)	0.004
Abdominal adiposity measures at 4.5 years								
SSAT (mL)	187	427.20 (251.24)	90	387.31 (203.40)	0.232	98	384.36 (197.41)	0.149
DSAT (mL)	187	173.88 (182.84)	90	137.85 (142.63)	0.171	98	135.33 (139.18)	0.132
VAT (mL)	187	192.02 (86.31)	90	188.35 (65.21)	0.473	98	190.55 (64.19)	0.454
Ectopic fat measured by MRS at 4.5 years								
Liver fat (% of liver weight)	158	0.567 (0.364)	96	0.560 (0.395)	0.689	86	0.588 (0.416)	0.273
Intramyocellular lipids (% of water content)	170	0.461(0.205)	107	0.514 (0.367)	0.009	92	0.520 (0.372)	0.008
Adiposity and metabolic parameters at 6 years								
Age (years)	198	6.05 (0.09)	116	6.04 (0.08)	0.154	593	6.06 (0.10)	0.447
Body mass index (kg/m^2)	198	15.70 (2.23)	116	15.59 (2.40)	0.962	591	15.53 (2.35)	0.961
Fatty liver index	84	1.100 (1.534)	50	1.135 (1.634)	0.719	203	1.55 (4.18)	0.099
Metabolic syndrome score	89	0.192 (2.262)	52	-0.095 (2.145)	0.585	215	0.00 (2.55)	0.278
Fasting plasma glucose (mmol/L)	142	4.51 (0.38)	92	4.48 (0.54)	0.053	348	4.55 (0.38)	0.978
Fasting plasma insulin (mU/L)	116	5.00 (3.94)	57	4.41 (2.30)	0.115	255	4.32 (2.95)	0.118

Data shown are N (%) for categorical variables and mean (SD) for continuous variables.

Abbreviations: BAT, brown adipose tissue; QC, quality control; DSAT, abdominal deep subcutaneous adipose tissue; FDSA, supraclavicular and axillary fat depot; SSAT, abdominal superficial subcutaneous adipose tissue; VAT, visceral adipose tissue.

[a]*P*-values are based on comparison of characteristics between study participants *vs* children excluded due to failed image quality control.

[b]*P*-values are based on comparison of characteristics between study participants *vs* children excluded due to nonparticipation in the whole GUSTO cohort.

and abdominal adiposity in all 3 ethnic groups, as well as in both boys and girls. Compared to Malay and Chinese children, the reduction in adiposity with increasing %BAT was greater among Indian children even though they had greater total and abdominal adiposity. Similarly, such associations were stronger in girls than in boys (Table 6).

Associations Between %BAT and Metabolic Profile at Age 4.5 Years and 6 Years

Each 1% unit increase in %BAT was associated with lower liver fat, −0.008 (−0.013, −0.003) by weight and lower IMCL, −0.003 (−0.006, −0.001) % of water (Table 5). Similarly, each 1% unit increase in %BAT at age 4.5 years was associated with lower FLI: −0.044 (−0.075, −0.013) and MetS score: −0.046 (−0.093, 0.001) at 6 years. There were no associations between %BAT and FPG or fasting plasma insulin concentrations (Table 5). Ethnicity and sex did not modify the association between %BAT and ectopic fat accumulation.

Associations Between FF of FD_{SA} and Metabolic Profile at Age 4.5 Years and 6 Years

Contrary to the associations between %BAT and metabolic profile, each 1% increase in FF within FD_{SA} had a positive association with higher total and abdominal adiposity, ectopic fat volumes, and metabolic parameters (Table 5). There was no association between FF and FPG or fasting plasma insulin concentrations.

Discussion

In this study, using water-fat MRI, we identified and quantified BAT in supraclavicular and axillary regions without physiological activation in 4.5-year old Asian children. We

Table 4. Correlations of percentage brown adipose tissue and brown adipose fat-signal-fraction with adiposity and metabolic profile of children

	N	Brown adipose tissue (%)		Brown adipose tissue fat-signal-fraction	
		Pearson correlation	*P*	Pearson correlation	*P*
Adiposity measures at 4·5 years					
Body mass index (kg/m^2)	198	−0.386	<0.001	0.422	<0.001
Sum of skinfold thickness (mm)	195	−0.483	<0.001	0.503	<0.001
SSAT (mL)	187	−0.487	<0.001	0.515	<0.001
DSAT (mL)	187	−0.486	<0.001	0.480	<0.001
VAT (mL)	187	−0.537	<0.001	0.426	<0.001
Ectopic fat at 4·5 years					
Liver fat measured by MRS (% of liver weight)	158	−0.194	0.014	0.181	0.023
Intramyocellular lipids (% of water content)	170	−0.166	0.031	0.188	0.014
Metabolic parameters at 6 years					
Fatty liver index	84	−0.305	0.005	0.348	0.001
Metabolic syndrome score	89	−0.194	0.069	0.298	0.005
Fasting plasma glucose (mmol/L)	142	−0.060	0.477	0.036	0.669
Fasting plasma insulin (mU/L)	116	−0.092	0.328	0.135	0.148

Two-sided *P*-values less than 0.05 are considered significant.
Abbreviations: DSAT, abdominal deep subcutaneous adipose tissue; SSAT, abdominal superficial subcutaneous adipose tissue; VAT, visceral adipose tissue.

observed an inverse relationship between %BAT and total adiposity, abdominal adipose tissue compartment volumes using MRI, ectopic fat accumulation in the liver and soleus muscle tissue using MRS and FLI. The accumulation of abdominal fat and ectopic adipose tissue is recognized as one of the important characteristics of obesity and a major risk factor of cardiometabolic diseases and has been shown to have an inverse relationship with BAT (9). In the past few years, multiple studies in animal and adult humans have convincingly showed that adult humans have functional BAT, which can be activated and which has the capacity for obesity-reducing thermogenesis (4). These observations of an inverse relationship with BAT at a non-activated state and metabolic risk markers underscore and support the favorable and important role of BAT in the pathophysiology of obesity.

We found that ethnicity and sex modify the associations between %BAT and adiposity. Compared to Malay and Chinese children, the strength of the associations was stronger in Indian children even though they had the highest degree of adiposity and most ectopic fat. The underlying mechanism for this observation is not known. However, our findings of ethnic differences in adiposity and IMCL is consistent with previous findings in the GUSTO cohort (21,27). We have previously shown interethnic variations in insulin sensitivity. With increasing adiposity, insulin sensitivity was generally lower, but the effect was less in Indians despite a greater extent of DSAT and IMCL accumulation compared to Chinese and Malays (28). These observations suggest that the presence of higher %BAT may not be as protective against adiposity in Indians as in the other 2 ethnic groups. To our knowledge, there is no study exploring sex differences in the association between BAT and adiposity. Several studies have suggested that women have greater activated BAT mass and activity than men (29-32). Pfannenberg et al reported that higher BAT mass and activity were observed in women older than 43 years, but no sex difference was observed in the younger age group (11-43 years) (33). Our finding of girls having lower %BAT is consistent with a recent study that observed lower cold-activated BAT mass in younger women (18-35 years) than men. The lower %BAT and the greater strength of association between %BAT and adiposity observed in girls may reflect that girls may benefit more from the protective effect of BAT compared to boys. The underlying mechanisms behind these ethnic and sex differences are not clear. However, these findings highlight that the potential protective effect of BAT, even in the nonactivated state, on adiposity may differ across ethnic groups and sex. This information is important as there is currently considerable ongoing focus on BAT as a therapeutic target for treatment of obesity.

The observed inverse relationship between %BAT and liver fat supports the potential role of BAT in the development of NAFLD. Possible mechanisms underlying these findings have been discussed previously (34-36). The oxidation of fatty acids in BAT inhibits lipid trafficking into the liver leading to suppression of liver fat accumulation and

Table 5. Association of percentage brown adipose tissue and fat-signal-fraction with metabolic parameters of children at 4.5 years and 6 years

Dependent variables	Percentage brown adipose tissue			Brown adipose tissue fat-signal-fraction		
	β (95% CI)	*P*	Corrected *P*	β (95% CI)	*P*	Corrected *P*
Adiposity measures at 4.5 years						
Body mass index (kg/m^2)	−0.08 (−0.10, −0.06)	<0.001	<0.001	0.20 (0.15, 0.25)	<0.001	<0.001
Sum of skinfold thickness (mm)	−0.57 (−0.70, −0.44)	<0.001	<0.001	1.35 (1.03, 1.67)	<0.001	<0.001
SSAT (mL)	−11.16 (−13.87, −8.45)	<0.001	<0.001	28.09 (21.58, 34.60)	<0.001	<0.001
DSAT (mL)	−8.21 (−10.17, −6.25)	<0.001	<0.001	19.19 (14.35, 24.03)	<0.001	<0.001
VAT (mL)	−4.26 (−5.19, −3.32)	<0.001	<0.001	8.16 (5.70, 10.62)	<0.001	<0.001
Ectopic fat measured by MRS at 4.5 years						
Liver fat (% of liver weight)	−0.008 (−0.013, −0.003)	0.004	0.007	0.017 (0.004, 0.029)	0.009	0.012
Intramyocellular lipids (% of water content)	−0.003 (−0.006, −0.001)	0.020	0.030	0.009 (0.002, 0.015)	0.009	0.011
Metabolic parameters at 6 years						
Fatty liver index	−0.044 (−0.075, −0.013)	0.005	0.008	0.117 (0.045, 0.189)	0.002	0.003
Metabolic syndrome score	−0.046 (−0.093, 0.001)	0.054	0.066	0.158 (0.051, 0.266)	0.004	0.007
Fasting plasma glucose (mmol/L)	−0.004 (−0.010, 0.002)	0.165	0.182	0.007 (−0.006, 0.021)	0.294	0.186
Fasting plasma Insulin (mU/L)	−0.032 (−0.101, 0.037)	0.362	0.362	0.118 (−0.051, 0.286)	0.169	0.294

Models were adjusted for ethnicity, sex, and age on MRI day. Coefficients (β) shown are differences in unit changes in adiposity and metabolic parameters with each 1% unit increase in percentage of brown adipose tissue. Two-sided *P*-values were determined with the use of multivariable regression models. *P*-values corrected using Benjamini-Hockberg method with false discovery rate of 0.05.
Abbreviations: DSAT, abdominal deep subcutaneous adipose tissue; SSAT, abdominal superficial subcutaneous adipose tissue; VAT, visceral adipose tissue.

thus consequently reduce the risk of developing NAFLD (34-36). Similarly, higher BAT activation measured by infrared thermography following cold exposure was associated with less liver fat and a more favorable metabolic profile in prepubertal children (37). We did not find an association between %BAT and glucose, insulin, and MetS scores in the children. As our study population of young children was relatively homogeneous, it is likely that fasting glucose and fasting insulin concentrations were still in the normal physiological range with less variation, enabling observations of significant differences.

Our findings add to the limited information on BAT in young children. Our study has several unique strengths. First, this study shows the novel finding of an inverse relationship between nonactivated BAT under thermoneutral conditions and metabolic profile in early childhood. The fact that these differences are observed in preschool-aged children points to underlying genetic and early environmental factors which has important future metabolic implications. Further, the GUSTO study draws from the 3 major Asian ethnic groups that represent 50% of the global population, increasing the relevance of these findings to global efforts to address noncommunicable diseases. Second, the mean age of the children in this study was 4.6 years, forming a homogenous age group unlike in most previous studies of BAT; thus, the observations on BAT can better represent preschool age. Moreover, the study participants were healthy and were not patients requiring PET/CT for medical indications. BAT activation can be interfered or altered in patients depending on the underlying disease status such as cancer and medication used which might lead to misinterpretation of the observations during PET/CT scans (38). Last, our findings strengthen the proposition of MRI as an alternative imaging technique to characterize BAT even in the nonactivated state. The available methods that identify BAT in humans are PET/CT and infrared thermography, and both only measure activated BAT, thus underestimating the presence of inactive or weakly activated BAT. Water-fat MRI does not use ionizing radiation or radioactive tracers; therefore, it can be used as a safe modality to identify BAT in future research in larger cohorts, longitudinal studies, and in the general population, especially in a pediatric population, to better understand the role BAT plays in humans.

There are some potential limitations that merit discussion. Water-fat MRI-derived measures of BAT either FF or volume, do not provide a direct measurement of BAT activity as PET/CT and does not differentiate between active and inactive BAT. Water-fat MRI is used by inference with the knowledge that lower FF in the supraclavicular-axillary region reflects BAT in the absence of pharmacological or cold stimulation (39,40). We acknowledge that information

Table 6. Association between percentage brown adipose tissue and adiposity measures at 4.5 years by ethnicity groups and sex

	BMI (kg/m^2)	ΣSFT (mm)	SSAT (mL)	DSAT (mL)	VAT (mL)
	β (95% CI)	β (95% CI)	β(95% CI)	β (95% CI)	β (95% CI)
Ethnicity[a]					
Chinese	−0.04 (−0.07,−0.01)	−0.31 (−0.45, −0.18)	−6.01 (−9.01, −3.01)	−4.49 (−6.66, −2.33)	−3.66 (−4.85, −2.48)
	$P = 0.010$	$P \leq 0.001$	$P \leq 0.001$	$P \leq 0.001$	$P \leq 0.001$
Malay	−0.06 (−0.09, −0.02)	−0.44 (−0.67, −0.21)	−8.79 (−13.34, −4.25)	−6.79 (−10.32, −3.26)	−2.35 (−3.58, −1.12)
	$P = 0.002$	$P \leq 0.001$	$P \leq 0.001$	$P \leq 0.001$	$P \leq 0.001$
Indian	−0.17 (−0.22, −0.12)	−1.19 (−1.51, −0.88)	−23.69 (−30.69, −16.69)	−17.21 (−21.89, −12.53)	−8.27 (−10.97, −5.57)
	$P \leq 0.001$	$P \leq 0.001$	$P \leq 0.001$	$P \leq 0.001$	$P \leq< 0.001$
P for interaction (ethnicity*%BAT)	$P \leq 0.001$	$P \leq 0.001$	$P \leq 0.001$	$P \leq 0.001$	$P \leq 0.001$
Sex[b]					
Girls	−0.09 (−0.12, −0.07)	−0.69 (−0.86, −0.52)	−13.28 (−16.78, −9.78)	−10.11 (−12.69, −7.52)	−4.71 (−5.87, −3.54)
	$P \leq 0.001$	$P \leq 0.001$	$P \leq 0.001$	$P \leq 0.001$	$P \leq 0.001$
Boys	−0.04 (−0.08, 0.00)	−0.31 (−0.52, −0.11)	−5.99 (−10.40, −1.57)	−3.56 (−6.53, −0.59)	−3.35 (−5.00, −1.70)
	$P = 0.049$	$P = 0.003$	$P = 0.009$	$P = 0.019$	$P \leq 0.001$
P for interaction (sex*%BAT)	$P = 0.038$	$P = 0.014$	$P = 0.030$	$P = 0.007$	$P = 0.223$

Coefficients (β) shown are differences in unit change in BMI, ΣSFT, SSAT, DSAT, and VAT with each 1% unit change in percentage of brown adipose tissue. Two sided P-values were determined with the use of multivariable regression models.

Abbreviations: BMI, body mass index; DSAT, abdominal deep subcutaneous adipose tissue; ΣSFT, sum of skinfold thickness; SSAT, abdominal superficial subcutaneous adipose tissue; VAT, visceral adipose tissue.

[a]Models adjusted for sex and age on MRI day.

[b]Models adjusted for ethnicity and age on MRI day.

based on FF alone may not have 100% sensitivity or specificity to draw this conclusion. However, as participants in this study are young children, either cold or pharmacological stimulation or more accurate methods involving radiation such as PET-CT would not be acceptable in our setting. Our approach is therefore based on findings from previous studies showing that BAT can be detected by water-fat MRI in a physiologic condition in comparison to PET/CT and validated by histology (15,41). In addition, at the present time, there are no standardized FF ranges or metrics for identifying BAT. It is not known if this range differs from cohort to cohort or by age and sex. In our study, FF was used as a broader range (ie, 20%-80%) based on FF identified as BAT in anatomical locations (supraclavicular and axillary fat depot) in previous studies for neonates, children, and adults (15,41,42). FF < 20% was excluded as such low FF represent FF from bones or muscle. In addition, the upper limit of the cutoff FF for BAT was considered based on FF of subcutaneous adipose tissue from MRS acquired in these children on the same day as BAT MRI was performed. The median FF of subcutaneous adipose tissue was 87.6% and the 10th percentile of FF was 80.8% (Fig. 4). Therefore, the chosen cutoff of 80% can be considered reasonable. Even selecting 80%, the heterogeneity of BAT at this age is such that underestimation of BAT is still a possibility especially for overweight or obese children in whom FF at FD_{SA} is higher (39). It is also possible that BAT in FD_{SA} may have a high FF that mimics WAT at the state before oxidation of stored lipids.

Only a subset of all GUSTO children was included in these analyses given the challenges of obtaining consent from parents, acquiring MRI in this age group, and stringent image quality control process. Although this number of subjects is the largest by far among BAT studies using water-fat MRI, caution is warranted in generalizing our findings. Future studies in a larger population as well as longitudinal studies are required to assess whether the observed associations persist. The secondary outcomes of this study, metabolic parameters in the blood, were measured at 6 years, approximately 1.5 years after MRI was performed. Therefore, the difference in temporal relationship between BAT and these metabolic markers may have attenuated the associations. Longitudinal follow-up of these children is ongoing to determine whether these associations persist. Last, in our regression models, we only controlled for factors that are known to be associated with BAT based on previous literature. Therefore, there may be residual confounding that may have affected our results.

In conclusion, our findings support the potential role of BAT in influencing adiposity and ectopic fat depots in Asian children. Observed ethnic and sex differences provide novel important information that the protective role of higher BAT may differ by ethnicity and sex. Long-term follow-up studies are warranted to replicate these findings to better understand the role of BAT and to determine the long-term health implications of BAT on the development of obesity and related metabolic disorders.

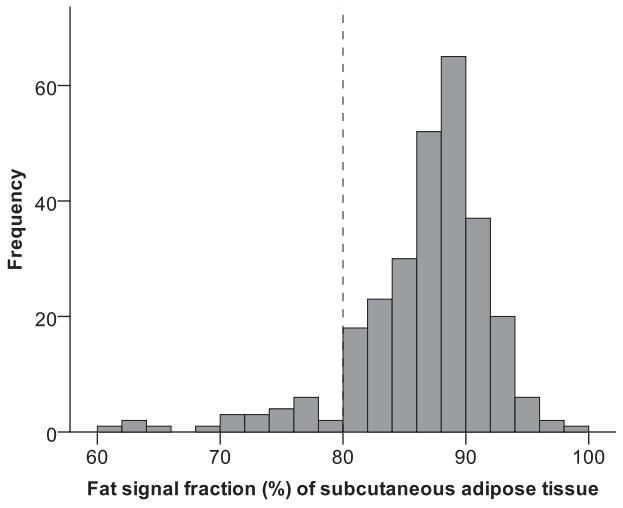

Figure 4. Histogram of fat-signal-fraction of subcutaneous adipose tissue in 4.5 years old children. Histogram of fat-signal-fraction of subcutaneous adipose tissue in 4.5 years old children from MRS acquired on the same day as water-fat MRI.

Acknowledgments

The authors thank Tan Ker Sin, Omar Mahmood and team, KKH Department of Diagnostic and Intervention Imaging for acquisition and postprocessing of water-fat MRI and Ivy Khin Thuzar Hlaing and Jay Jay Thaung Zaw for segmentation of brown adipose tissue image data sets. The authors also thank The GUSTO study group. The GUSTO study group includes Allan Sheppard, Amutha Chinnadurai, Anne Eng Neo Goh, Anne Rifkin-Graboi, Anqi Qiu, Arijit Biswas, Bee Wah Lee, Birit F.P. Broekman, Boon Long Quah, Borys Shuter, Chai Kiat Chng, Cheryl Ngo, Choon Looi Bong, Christiani Jeyakumar Henry, Claudia Chi, Cornelia Yin Ing Chee, Yam Thiam Daniel Goh, Doris Fok, E Shyong Tai, Elaine Tham, Elaine Quah Phaik Ling, Evelyn Chung Ning Law, Evelyn Xiu Ling Loo, Falk Mueller-Riemenschneider, George Seow Heong Yeo, Helen Chen, Heng Hao Tan, Hugo P. S. van Bever, Iliana Magiati, Inez Bik Yun Wong, Ivy Yee-Man Lau, Izzuddin Bin Mohd Aris, Jeevesh Kapur, Jenny L. Richmond, Jerry Kok Yen Chan, Joanna D. Holbrook, Joanne Yoong, Joao N. Ferreira., Jonathan Tze Liang Choo, Jonathan Y. Bernard, Joshua J. Gooley, Kenneth Kwek, Krishnamoorthy Niduvaje, Leher Singh, Lieng Hsi Ling, Lin Su, Ling-Wei Chen, Lourdes Mary Daniel, Mark Hanson, Mary Foong-Fong Chong, Mary Rauff, Mei Chien Chua, Michael Meaney, Oon Hoe Teoh, P. C. Wong, Paulin Tay Straughan, Pratibha Agarwal, Queenie Ling Jun Li, Rob M. van Dam, Salome A. Rebello, Seang-Mei Saw, See Ling Loy, Seng Bin Ang, Shang Chee Chong, Sharon Ng, Shirong Cai, Shu-E Soh, Sok Bee Lim, Stella Tsotsi, Chin-Ying Stephen Hsu, Sue Anne Toh, Swee Chye Quek, Victor Samuel Rajadurai, Walter Stunkel, Wayne Cutfield, Wee Meng Han, Wei Pang, Yin

Bun Cheung, and Yiong Huak Chan. Authors thank to mothers and children, and families who participated in GUSTO study.

Financial Support: This research is supported by the Singapore National Research Foundation under its Translational and Clinical Research (TCR) Flagship Programme and administered by the Singapore Ministry of Health's National Medical Research Council (NMRC), Singapore—NMRC/TCR/004-NUS/2008; NMRC/TCR/012-NUHS/2014. Additional funding is provided by the Singapore Institute for Clinical Sciences, Agency for Science Technology and Research (A*STAR), Singapore.

Author Contributions: M.T.T. contributed to data acquisition, image analysis of brown adipose tissue, analyses and interpretation the data, and writing the manuscript. H.H.H., K.J.L., and M.V.F. supervised image acquisition and image analysis. N.M., S.A.S., and S.S.V. performed analysis of MRI and MRS. J.H., C.Z., and J.G.E. provided statistical advice. P.D.G., Y.S.C., K.M.G., and J.G.E. conceptualized and designed this study. All authors contributed to discussion and revision of the manuscript for important intellectual content. All authors have read and approved the final manuscript. M.T.T. and J.G.E. had primary responsibility for the contents of the article.

Additional Information

Correspondence: Johan G. Eriksson, Department of Obstetrics and Gynaecology, Yong Loo Lin School of Medicine, National University of Singapore, MD1, Tahir Foundation Building, Level 12, #12-02/03, 12 Science Drive 2, Singapore 117549, Singapore. Email: obgjge@nus.edu.sg; johan.eriksson@helsinki.fi.

Disclosure Summary: Y.S.C., K.M.G., and S.Y.C. are part of an academic consortium that has received research funding from companies selling nutritional products. K.M.G. and S.Y.C. has received reimbursement for speaking at conferences sponsored by companies selling nutritional products. K.M.G. is supported by the UK Medical Research Council (MC_UU_12011/4), the National Institute for Health Research (NIHR senior investigator; NF-SI-0515-10042), NIHR Southampton 1000DaysPlus Global Nutrition Research Group (17/63/154) and NIHR Southampton Biomedical Research Centre (IS-BRC-1215-20004)), the European Union (Erasmus+ Programme Early Nutrition eAcademy Southeast Asia-573651-EPP-1-2016-1-DE-EPPKA2-CBHE-JP and ImpENSA 598488-EPP-1-2018-1-DE-EPPKA2-CBHE-JP), and the British Heart Foundation (RG/15/17/3174). All other authors declare no potential conflict of interest that might bias the submitted work and no other relationships or activities that could appear to have influenced the submitted work.

Data Availability: Some or all data sets generated during and/or analyzed during the current study are not publicly available but are available from the corresponding authors on reasonable request.

References

1. Rui L. Brown and beige adipose tissues in health and disease. *Compr Physiol*. 2017;**7**(4):1281-1306.
2. Bartelt A, Bruns OT, Reimer R, et al. Brown adipose tissue activity controls triglyceride clearance. *Nat Med*. 2011;**17**(2):200-205.
3. Arany Z. Taking a BAT to the chains of diabetes. *N Engl J Med*. 2019;**381**(23):2270-2272.
4. Townsend KL, Tseng YH. Brown fat fuel utilization and thermogenesis. *Trends Endocrinol Metab*. 2014;**25**(4):168-177.
5. Virtanen KA, Lidell ME, Orava J, et al. Functional brown adipose tissue in healthy adults. *N Engl J Med*. 2009;**360**(15):1518-1525.
6. Cypess AM, Lehman S, Williams G, et al. Identification and importance of brown adipose tissue in adult humans. *N Engl J Med*. 2009;**360**(15):1509-1517.
7. van Marken Lichtenbelt WD, Vanhommerig JW, Smulders NM, et al. Cold-activated brown adipose tissue in healthy men. *N Engl J Med*. 2009;**360**(15):1500-1508.
8. Gilsanz V, Smith ML, Goodarzian F, Kim M, Wren TA, Hu HH. Changes in brown adipose tissue in boys and girls during childhood and puberty. *J. Pediatr.* 2012;**160**:604-609.e601.
9. Brendle C, Werner MK, Schmadl M, et al. Correlation of brown adipose tissue with other body fat compartments and patient characteristics: a retrospective analysis in a large patient cohort using PET/CT. *Acad Radiol*. 2018;**25**(1):102-110.
10. Green AL, Bagci U, Hussein S, et al. Brown adipose tissue detected by PET/CT imaging is associated with less central obesity. *Nucl Med Commun*. 2017;**38**(7):629-635.
11. Robinson L, Ojha S, Symonds ME, Budge H. Body mass index as a determinant of brown adipose tissue function in healthy children. *J. Pediatr.* 2014;**164**:318-322.e311.
12. Gifford A, Towse TF, Walker RC, Avison MJ, Welch EB. Characterizing active and inactive brown adipose tissue in adult humans using PET-CT and MR imaging. *Am J Physiol Endocrinol Metab*. 2016;**311**(1):E95-E104.
13. Carpentier AC, Blondin DP, Virtanen KA, Richard D, Haman F, Turcotte ÉE. Brown adipose tissue energy metabolism in humans. *Front Endocrinol (Lausanne)*. 2018;**9**:447.
14. Din MU, Saari T, Raiko J, et al. Postprandial oxidative metabolism of human brown fat indicates thermogenesis. *Cell metab*. 2018;**28**:207-216.e203.
15. Hu HH, Perkins TG, Chia JM, Gilsanz V. Characterization of human brown adipose tissue by chemical-shift water-fat MRI. *AJR Am J Roentgenol*. 2013;**200**(1):177-183.
16. Hu HH, Yin L, Aggabao PC, Perkins TG, Chia JM, Gilsanz V. Comparison of brown and white adipose tissues in infants and children with chemical-shift-encoded water-fat MRI. *J Magn Reson Imaging*. 2013;**38**(4):885-896.
17. Andersson J, Roswall J, Kjellberg E, Ahlström H, Dahlgren J, Kullberg J. MRI estimates of brown adipose tissue in children: associations to adiposity, osteocalcin, and thigh muscle volume. *Magn Reson Imaging*. 2019;**58**:135-142.
18. Soh SE, Tint MT, Gluckman PD, et al; GUSTO Study Group. Cohort profile: Growing Up in Singapore Towards healthy Outcomes (GUSTO) birth cohort study. *Int J Epidemiol*. 2014;**43**(5):1401-1409.
19. Taha AA, Hanbury A. Metrics for evaluating 3D medical image segmentation: analysis, selection, and tool. *BMC Med Imaging*. 2015;**15**:29.
20. Sadananthan SA, Prakash B, Leow MK, et al. Automated segmentation of visceral and subcutaneous (deep and superficial) adipose tissues in normal and overweight men. *J Magn Reson Imaging*. 2015;**41**(4):924-934.
21. Sadananthan SA, Tint MT, Michael N, et al. Association between early life weight gain and abdominal fat partitioning at 4.5 years is sex, ethnicity, and age dependent. *Obesity* 2019;**27**:470-478.

22. Bedogni G, Bellentani S, Miglioli L, et al. The Fatty Liver Index: a simple and accurate predictor of hepatic steatosis in the general population. *BMC Gastroenterol*. 2006;**6**:33.
23. Ahrens W, Moreno LA, Mårild S, et al; IDEFICS consortium. Metabolic syndrome in young children: definitions and results of the IDEFICS study. *Int J Obes (Lond)*. 2014;**38**(Suppl 2):S4-14.
24. Matthews DR, Hosker JP, Rudenski AS, Naylor BA, Treacher DF, Turner RC. Homeostasis model assessment: insulin resistance and beta-cell function from fasting plasma glucose and insulin concentrations in man. *Diabetologia*. 1985;**28**:412-419.
25. Benjamini Y, Hochberg Y. Controlling the false discovery rate: a practical and powerful approach to multiple testing. *J R Stat Soc Series B (Methodological)*. 1995;**57**:289-300.
26. Cole TJ, Bellizzi MC, Flegal KM, Dietz WH. Establishing a standard definition for child overweight and obesity worldwide: international survey. *BMJ*. 2000;**320**(7244):1240-1243.
27. Michael N, Gupta V, Sadananthan SA, et al. Determinants of intramyocellular lipid accumulation in early childhood. *Int J Obes*. 2020;**44**(5):1141-1151.
28. Khoo CM, Leow MK, Sadananthan SA, et al. Body fat partitioning does not explain the interethnic variation in insulin sensitivity among Asian ethnicity: the Singapore adults metabolism study. *Diabetes*. 2014;**63**(3):1093-1102.
29. Au-Yong IT, Thorn N, Ganatra R, Perkins AC, Symonds ME. Brown adipose tissue and seasonal variation in humans. *Diabetes*. 2009;**58**(11):2583-2587.
30. Zhang Z, Cypess AM, Miao Q, et al. The prevalence and predictors of active brown adipose tissue in Chinese adults. *Eur J Endocrinol*. 2014;**170**(3):359-366.
31. Perkins AC, Mshelia DS, Symonds ME, Sathekge M. Prevalence and pattern of brown adipose tissue distribution of 18F-FDG in patients undergoing PET-CT in a subtropical climatic zone. *Nucl Med Commun*. 2013;**34**(2):168-174.
32. Yeung HW, Grewal RK, Gonen M, Schöder H, Larson SM. Patterns of (18)F-FDG uptake in adipose tissue and muscle: a potential source of false-positives for PET. *J Nucl Med*. 2003;**44**(11):1789-1796.
33. Pfannenberg C, Werner MK, Ripkens S, et al. Impact of age on the relationships of brown adipose tissue with sex and adiposity in humans. *Diabetes*. 2010;**59**(7):1789-1793.
34. Poekes L, Legry V, Schakman O, et al. Defective adaptive thermogenesis contributes to metabolic syndrome and liver steatosis in obese mice. *Clin Sci (Lond)*. 2017;**131**(4):285-296.
35. Yilmaz Y, Ones T, Purnak T, et al. Association between the presence of brown adipose tissue and non-alcoholic fatty liver disease in adult humans. *Aliment Pharm Ther*. 2011;**34**:318-323.
36. Chondronikola M, Volpi E, Børsheim E, et al. Brown adipose tissue activation is linked to distinct systemic effects on lipid metabolism in humans. *Cell Metab*. 2016;**23**(6):1200-1206.
37. Malpique R, Gallego-Escuredo JM, Sebastiani G, et al. Brown adipose tissue in prepubertal children: associations with sex, birthweight, and metabolic profile. *Int J Obes (Lond)*. 2019;**43**(2):384-391.
38. Steinberg JD, Vogel W, Vegt E. Factors influencing brown fat activation in FDG PET/CT: a retrospective analysis of 15 000+ cases. *Br J Radiol*. 2017;**90**(1075):20170093.
39. Deng J, Schoeneman SE, Zhang H, et al. MRI characterization of brown adipose tissue in obese and normal-weight children. *Pediatr Radiol*. 2015;**45**(11):1682-1689.
40. Kistner A, Rydén H, Anderstam B, Hellström A, Skorpil M. Brown adipose tissue in young adults who were born preterm or small for gestational age. *J Pediatr Endocrinol Metab*. 2018;**31**(6):641-647.
41. Gifford A, Towse TF, Walker RC, Avison MJ, Welch EB. Human brown adipose tissue depots automatically segmented by positron emission tomography/computed tomography and registered magnetic resonance images. *J Vis Exp*. 2015;18;(96):52415.
42. Rasmussen JM, Entringer S, Nguyen A, et al. Brown adipose tissue quantification in human neonates using water-fat separated MRI. *PLoS One*. 2013;**8**(10):e77907.